The light-tightness of the shutter box and instilation of the NEG Ion-getter pump for ALPS-II

Sarah Larkin, Univerty College Dubin, Ireland

September 29, 2014

Abstract

The light-tightness of the aluminium shutter box, which is to be used in ALPS-II at DESY, was tested. The shutter box is connected to an aluminium breadboard by a notch/ groove. The light tightness of the notch/groove was tested. The test was done using an SBIG ST-402ME CCD camera. In the first set up the box was above the breadboard and in the second the breadboard was sitting on top of the box set up. It was found 0.010435 $\pm$0.00102 were leaked into the box over a 1800 seconds exposure time. This was a factor of 14.81 more photon/pixel/second compared to having only the connection between the box and CCD camera test. The shutter on the shutter box was also tested for light tightness. It was found that the shutter was not light tight. To test for the light leakage dependency on exposure time, the count intensity was plotted as a function of time. It was found that the light leakage increased by 0.0067 counts/second.

The performance test of a costume build NEG/Ion getter pump was carried out. This pump was used in previous experiment in DESY and to verify that it would be suitable for ALPS-II. It performance need to be test before being installed. A vacuum pressure of $\sim 10^{-10}$ mbar was achieved and it is planed to install the pump to the second cavity of ALPS-II.

Contents

1 Introduction

One of the most interesting topics in science is the fundamental understanding of our universe. There is a number of strongly supported theoretical proposals stating that the Standard Model (SM) of elementary particle physics is incomplete. Currently the SM theory is unable to describe the particles and the interaction that make up all matter, as we are still trying to observe and measure the fundamental particle or particles that make up Dark Matter.

One of the motivated extensions to the SM is weakly-interacting slim particles(WISPs). The axion is a prime example of a WISP and is predicted to solve the strong CP problem and axions and axion-like particles are considered as a strong candidate for cold Dark Matter. The Axion or ALPs would interact extremely weakly with the known matter and with a mass of around 1 meV an axion could make up the uncounted mass of the Universe.

In Deutshes Electronen-Synchrotron (DESY), Hamburg, Germany, the Any Light Particle Search ALPS group searched for ALPs by investigating photon-WISP interactions. In 2010 the ALPS-I experiment was able to set the limits of the probability of the photon-WISP-photon conversion of a few $\times 10^{-25}$. After the success of ALPS-I, ALPS-II is currently under construction. The aim of ALPS-II is to detect low mass-axion-like particles which will lead to a better understanding of are universe.

2 Theory

The is a number of different experimental set ups used to detect WISPS, there is purely laboratory experiments such as light-shinning-through-wall (LSW), Helioscopes [1] and Haloscopes [2].

In ALPS the LSW set-up is used. The experiment is based on photon-WISP-photon conversion and the theory that a WISP due to its very weak interaction with SM constituents could pass through standard matter, which in this case is a wall.

A photon can be converted in to a WISP by kinetic mixing (hidden photons) or by the Primakoff effect (axion-like particles)

Hidden sectors are predicted e.g. by string theory and consist of unobserved gauge bosons which are separate from SM gauge bosons. The hidden photon acts as a messenger particle between the hidden sector and the SM sector. It couples to the hidden sector and to the electromagnetic current of the SM photon by kinetic mixing resulting in vacuum oscillations in between them [3]. The Lagrangian density for this iteration is:

$$\mathscr{L}_{\mathtt{int}} = -\frac{\chi}{2} F_{\mu\nu} B^{\mu\nu} \tag{1}$$

where $B_{\mu\nu}$ is the HP field-strength and χ is the kinetic mixing.

The Primakoff effect is the conversion of an axion into photons and vice versa in the presence of a strong magnetic field perpendicular to the direction of propagation of the axion. See Figure 1.

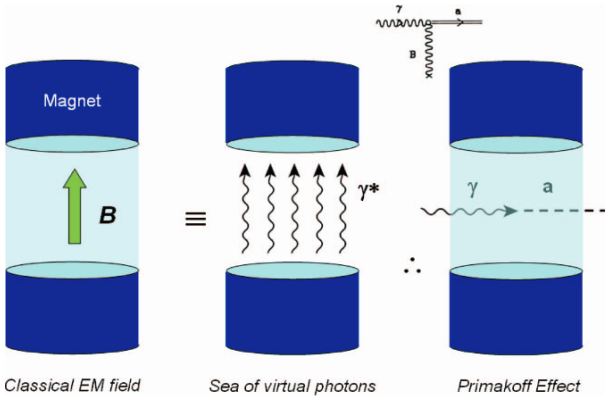

Figure 1: One may treat a classical electromagnetic field as a sea of virtual photons, and thus an axion may convert into a single real photon carrying the full energy mass plus kinetic of the axion. The same is true for the inverse process of a photon converting into an axion. The external electromagnetic field assures the conservation of momentum. Picture taken from [5]

The Lagrangian density for this coupling is:

$$\mathscr{L}_{\mathtt{int}} = \frac{1}{4} g_{\phi\gamma} \phi F_{\mu\nu} \tilde{F}_{\mu\nu} \tag{2}$$

where ϕ is the axion, $g_{\phi\gamma}$ is the coupling constant and $F_{\mu\nu}$ is the electromagnetic tensor.

$$g_{\phi\gamma} = \frac{\alpha}{2\pi f_a} \left(\frac{E}{N} - 1.92 \pm 0.008 \right) \tag{3}$$

where α is the fine structure constant, f_a is the symmetry breaking scale, and E and N , respectively are the electromagnetic and colour anomaly of the axial current associated with the axion field.

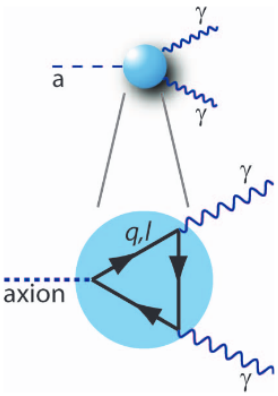

Figure 2: The axion is a pseudoscalar particle, a light cousin to the neutral pion, and couples to two photons via a loop of charged fermions. [5]

The probability of a photon-WISP conversion is given as :

$$P_{\gamma\to\phi} = \frac{g_{\phi\gamma}^2}{4}(BL)^2\frac{\sin^2(qL/2)}{(qL/2)^2} \tag{4}$$

where L is the length of the magnetic filed, B is the magnetic field strength and q = $m_\phi/2E_\gamma$ the WISP-photon momentum difference. The probability of a photon-WISP-photon conversion is given as:

$$P_{\gamma\to\phi\to\gamma} = P_{\gamma\to\phi}(B_1, l_1, q_1)P_{\phi\to\gamma}(B_2, l_2, q_2) \tag{5}$$

$$P_{\gamma\to\phi\to\gamma} \sim g^4 \tag{6}$$

The probability is maximal if the axion and photon remain in phase over the magnet length i.e. when the qL << π.

For sensitivity to higher axion masses, the conversion region must be filled with a buffer gas such as argon which provides an effective photon mass m_γ. Giving a conversion probability of

$$P_{\phi\to\gamma} = \left(\frac{Bg_{a\gamma}}{2}\right)^2 \frac{1}{q^2+\Gamma^2/4}\left(1 + e^{-\Gamma L} - 2e^{-\Gamma L/2}\cos(qL)\right) \tag{7}$$

where q=$|m_a^2 - m_\gamma^2|/2E_a$ and Γ is the inverse absorption length for photons in a gas [4].

In ALPS-I the length of the magnet was 10 meters while at the final build of ALPS-II the length of the magnet string will be 100 meters and thus the probability of detecting a photon-WISP-photon interaction would be increased.

3 ALPS-I

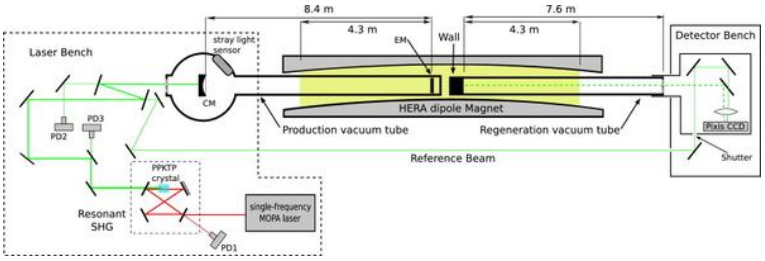

Figure 3: Layout of the ALPS-I [7]

As shown in figure[3] at one end a laser beam entered generation tube of the magnet which contain a optical cavity. The beam oscillated between two mirrors before hitting the ″wall". The wall absorbed any photons leaving the cavity while WISP would penetrate through the wall into the regeneration tube. The regenerated photons are re-directed by an oblique mirror to the PIXIS 1024B CCD camera. The dark current were 0.001 e/pixels.s and the read out noise was 3.8 e/pixel RMS. Only 1 hour exposure frame could be taken due to an increase of exposure time will increase the probability of comic or radioactive signal close to the expected 30 μm beam.

After the experiment's final upgrade the collaboration limits on the probability of photon-WISP-photon conversions of a few $\times 10^{-25}$ which was the most stringent laboratory constraints on the existence of ALPs and hidden photons.

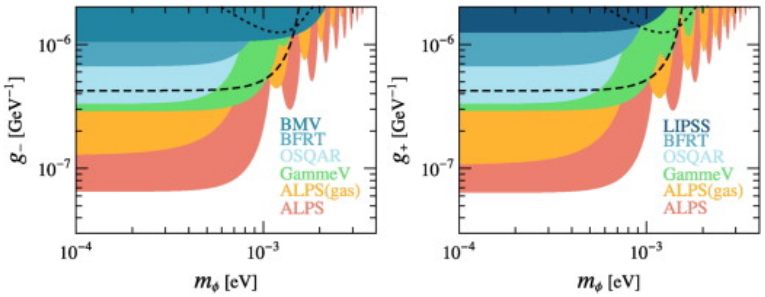

Figure 4: Exclusion limits (95 % C.L.) for pseudoscalar (left) and scalar (right) axion-like-particles from ALPS I compared to other laboratory experiments [6]

4 ALPS-II Proposal

The ALPS-II experiment is currently held near the HERA tunnel in DESY. It is in this first stage of a two stage build. In the second stage the experiment will be moved to the

HERA tunnel in 2018.

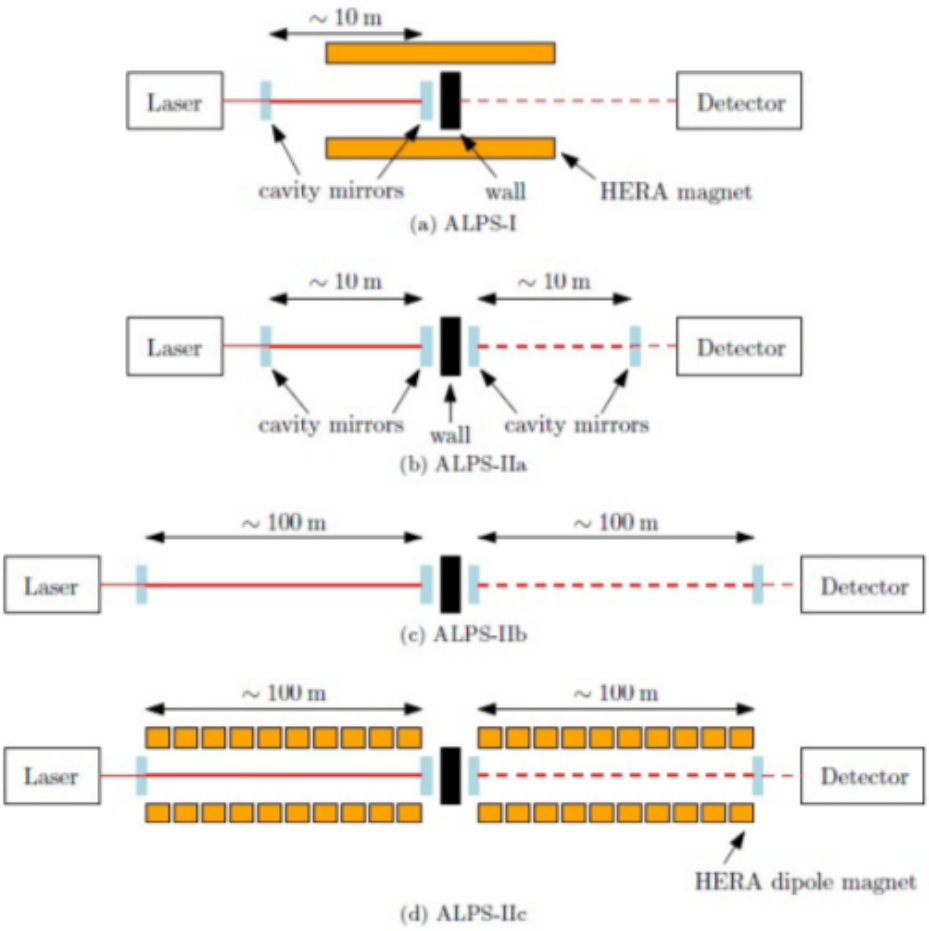

Figure 5: a) The set up of ALPS-I, b) First stage of ALPS-II build, c) An intermediate build which due to budgeting will be skipped, d) Final stage of the build

Figure 5 b) shows the set-up of the first stage of the build. At the end of this stage the Nd:YAG laser with a wavelength of 1064 nm and the two laser cavities either side of the wall both about 10 meters long will be set up. The laser, optical cavities and the detector will be tested and characterised. At this stage of the set up hidden photons would be detectable and therefore even in the first stage shining-through the wall particle could be detected.

Figure 5 d) show the final set up. The two cavities will be both about 100 meters long and the magnetic dipoles used form the HERA experiment with a magnetic field of 5 T or approximately 1000 Tm will surround the cavities. Only at this stage would it be possible to detect for Axions and ALPs due to the presence of the magnetic field.

20 (10 per cavity) HERA dipole magnets will be straightened by forcing deformation form the outer vacuum vessel at the 3 planes of the dipoles [7].

Detection for ALPS-II will be carried out using a Transition-Edge Sensor (TES) unlike ALPS-I which used the a PIXIS 1024B CCD camera. Transition-edge sensors using the rapid change of the resistance at super conducting phase transition. Unlike AlPS-I, ALPS-II is using an infra-red light source and the PISXIS has a poor quantum efficiency for the infra-red region while the has high sensitivity and a high quantum efficiencies in this region.

ALPS-I's refractive index in the optical resonators was changed by injecting Argon gas into the vacuum pipe. At ALPS-IIc Helium gas will be used as the wall of the vacuum pipe will be at the liquid Helium temperature causing gases to condensate on the cold surface. The Helium can also condensate, but the pressure build up is still high enough to meet the experiment's allowed standard.

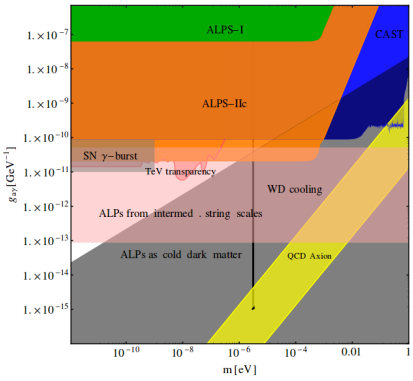

Figure 6: Schematic overview of the sensitity reach of the final stage of ALPS-II [7]

5 The test for Light-tightness of the shutter-box

The shutter on the shutter-box will acts as the "wall" for the LSW set up. The shutter box will hold one of the regeneration cavity mirrors and mirrors to redirect the green laser from the angled dichronic to the regeneration cavity. It is also where the any regenerated photons will be redirected to the detector. A shutter is needed so that the lasers could be aligned (see appendix figure 24 for layout of the shutter box). Light-tightness of this vessel is essential in order to isolate regenerated photons from photon outside the experiment.

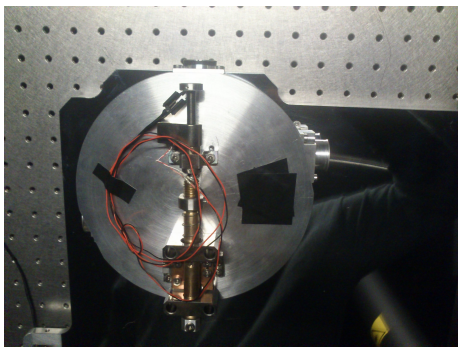

Figure 7: Shutter box from above with the motor for the shutter attached

The box is held in place by a groove in the aluminium breadbroad. The aim of my experiment was to test for the light-tightness of this groove and the light-tightness of the shutter. A SBIG CCD Camera was used to measure this light-tightness.

5.1 CCD Camera

In this experiment Charge-Coupled Device (CCD) Detectors were used at various stages in the build to test for light - tightness of the set-up. To insure that the detection of infra-red photons are from a WISP-photon iteration all other spurious photon must be minimized.

A CCD is a silicon wafer divided into an array of thousand of Metal Oxide Semiconductors (MOS) capacitor used as photodiode and storage device. A MOS device has reverse bias operation, causing the negatively charged electron to move to an area under the positively charged electrode strips or gates deposited on the chip. Electrons liberated by photon interaction are stored on the depletion region up to the full well reservoir capacity.

The MOS structure are segregated in one dimensional voltages applied to the surface electrodes and electrically isolated in the other direction by channel stops or insulating barriers, within the silicon substrate.

Incident photons are absorbed by the MOS structures causing electrons to be liberated forming electron-deficient sites (holes) in the silicon lattice. An electron-hole pair is generated by each absorbed photon , therefore accumulated charge in each pixel is linearly proportional to the number of incident photons.

During readout the collected charge is shifted along the transfer channels to the readout node. The collected charge move from regions of higher to lower potential region controlled by the applied voltage on the capacitor gate. This movement of charge is done in rows and at the last row of the potential wells the charge is then shifted to

the serial register. The charge is then stored into a coupled storage array in the overlying electrode structure. Then the pixels are read out in discrete packets until all are read.

The SBIG ST-402 uses a CCD architecture to move charge from the register to the readout amplifier called Frame Transfer. The photoactive area is divided from the light shield array where the electronic data are stored and transferred to the serial register. The shielded or masked array is only about 8 pixels rows in the x direction and y rows in the y direction. This architecture allows the initial frame to be stored in the storage array while the image array integrates charge for the next frame.

The wells of parallel register clocks independently shift charge on the image or the storage array. Therefore the CCD does not need a shutter at the charge transfer process and thus increase the frame rate compared to other architectures such as Full Frame CCD architectures.

After the output amplifier the signal is transmitted to an analog-to-digital converter(ADC) which converts the voltage value into a binary code which is read by the computer. Each pixel is assigned a digital value corresponding to signal amplitude in steps sized according to the bit depth of the ADC. Each step is called an analog-to-digital unit (ADU). The SBIG-402 has a 16-bit resolution resulting in any pixel having a value from 0 to 65,535 ADU. This values are sometimes known as the grey level steps. The number of accumulated photoelectrons determine the level step. This step is known as the electronic gain.

When operating a CCD camera the signal-to-noise ratio (SNR) of the camera must be known in order to determine its sensitivity. This ratio measures the signal levels that can be detected in an exposure. The sensitivity depends on the limiting noise factor. The signal is determined as a product on input light level, quantum efficiency and integration time in seconds.

CCD noise can be generated by system noise, thermal noise (dark current) and readout noise. System noise is caused by the readout amplifier noise and dark noise is the result of kinetic vibrations of the silicon atoms in the silicon chip that liberate electrons or holes even when the device is in total darkness. The dark noise is dependent on the temperature of the chip and therefore most CCD cameras have a cooling system to reduce the temperature of the chip and to keep it constant though out there exposure.

Readout noise is caused by the on-chip preamplifer during the process of converting charge carriers onto a voltage signal. It can be can be divided in to two types of noise, white and flicker noise. White noise comes for the metal oxide semiconductor field effect transistor of the output amplifier where the transistor resistance generates thermal noise. Flicker noise is the result of the material interface between the silicon and silicon diode layers of the array elements.

In order to eliminate these noise signals, an overscan (i.e. reading more pixels than exist) is used to measure the read out noise. The overscan is averaged and this average is subtracted from each frame. A dark frame (i.e. a frame of the same exposure length as the signal frame but with shutter of the camera closed) is taken. A number of dark frames are taken and are averaged giving the measured dark current noise. This is then subtracted from the signal frame giving the corrected signal frame.

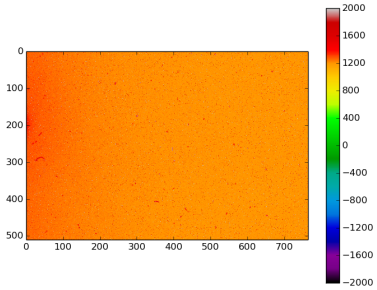

(a)
Dark Frame:
This matix of the readout pixels shows a count intensity in the order of 10^3 over all on the chip and a even higher intensity the left of the chip. This high count is due to read out noise due to the mechanics of the chip being read.

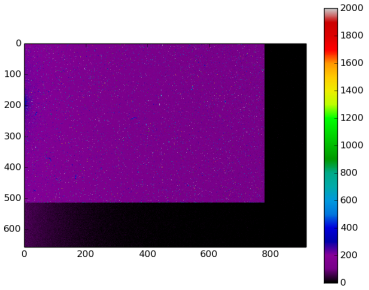

(b) Corrected Dark Frame:
The noise is corrected by using a over scan method and virtual pixels are measured, averaged and subtracted form the real image. The count intensity drop by an order of magnitude

The Quantum efficiency (QE) is the measure of the probability of a photon having a particular wavelength will be captured and liberate a charge carrier. The interaction between a photon and the detector depends on the detectors spectral sensitivity range. The SBIG has a QE has a pick QE of 83 percent at about 640 nm.

The shutter-box examined in this report is the upgrade of a previous shutter box design. Previously the set up was that the shutter box would sit on the breadboard by two smaller notches.

5.2 Breadboard below shutter-box

The set up of the first light tightness test was done as shown in diagram 9. The light source used in the test was the clean room light bulb and a 10 Watt LED lamp . The lamp was placed on the right hand side of the shutter box for all readings.

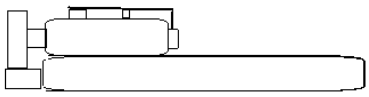

(a) The shutter box was place on top of the bread board and the SBIG was placed at the port opposite the shutter

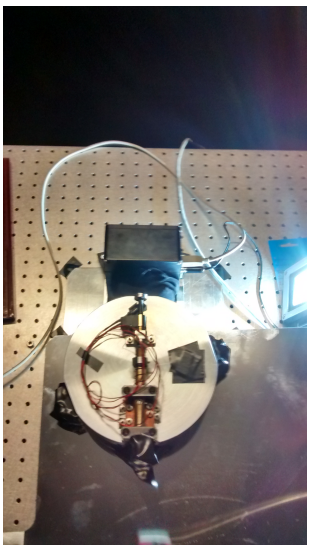

(b)

Figure 9: First Set up

The CCD camera was attached using a connection (see appendix figure 23) and was held in place by black tape to the shutter box. The three remaining ports (including the port for the shutter) were sealed form the inside.

Using the SBIG ST-402ME (see appendix for specification sheet) and CDDOP version 5 frames at different exposure times were taken. 10 dark frames were taken at 1800 seconds of exposure, respectively. These frames were summed together and averaged to get the Master dark frames. With all four ports sealed from the inside. 1800 seconds of exposure with the CCD shutter open was taken to test the light-tightness of the connection. It was found that the connection was light tight.

The inside tape at the connection was removed and another 1800 seconds of exposure with the CCD shutter open were taken. This would show the light-tightness of the groove of the box. The result showed that the groove was not light-tight.

The connection was then retested and it was found no longer to be light-tight.

Therefore it was hypothesised that lifting the box to remove the tape meant that the connection was distorted and the light-tightness of the connection was distorted. Thus, we thought of a different set-up.

5.3 Breadboard above shutter-box

A second set up was used as shown in figure 10.

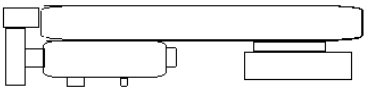

(a) The bread was place on top of the shutter box and the breadboard was stabilized by items found in the lab

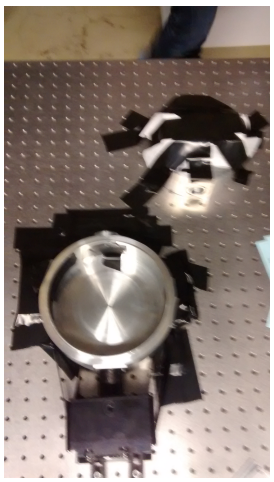

(b)

Figure 10: Second Set up

This meant that the only the breadboard could be lifted to get access to the inside of the box and the connection would not distorted.

After the first run it was found that the set up was not stable and the result were not reproducible therefore the set up was upgrade to a new set up 11.

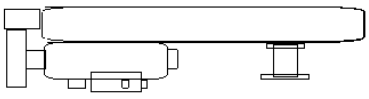

(a) The set up as before except the breadboard was stabilise using a stand that could be higher or lower in terms of millimetres and metal items add to hold the box itself in place

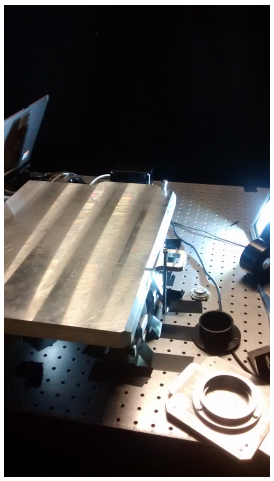

(b)

Figure 11: Final Set up

The connection was retested for light tightness, followed by the groove.

6 Results

A software called CCDOP version 5 was used to operate the SBIG camera. This software stored the ADU counts in a 2D matrix in a FIG file. A Python 2.7 code was used to analysis this files (see appendix Listing 1).

Exposure time of 1800 seconds was determined to be the ideal time length to test of light-tightness, as ALPS-II measure runs will be in the order of 10^3 seconds and 1800 seconds would be long enough to test the light leakage at this order. A longer exposure was not possible due to time constraints.

It was found that when one computes counts/seconds one sees that the shutter lets in additional light. See table 1.

As little was know about the light source i.e. the room-light which was a dark body radiation and the LED lamp used, multiple exposure times were taken to test for constancy of the light source. Also rate of counts over time was analysed. For each measurement the minimum, maximum and average count for the corrected frame during the exposure in ADU where calculated.

Photon per pixel per second was calculated using the equation:

$$P = \frac{\texttt{counts} \times \texttt{gain}}{\texttt{exposure time}} \tag{8}$$

The following result were taken using the final set-up.

Table 1: Result of Light-tightness for final set-up

	Connection	Groove			Shutter
Exposure [seconds]	1800	1800	180	18	300
Count minimum	-3766.77	-49399.1	-1062.07	-103.707	-3408.26
Count maximum	46184.9	30737.1	1119.93	1281.29	4882.74
Count mean	0.794783	12.5167	1.87474	0.26265	9.31611
Count Std.	1.221637	1.2265	0.51157	0.49954	0.04658
Photon/pix/sec	0.00066	0.010435	0.01562	0.021888	0.65900
Photon/pix/sec Std.	0.00102	0.00102	0.00426	0.041629	0.00329

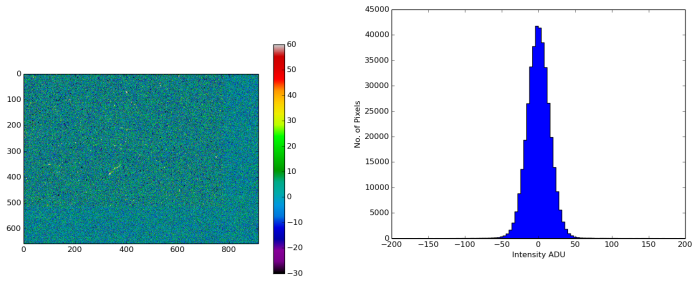

(a) (b)

Figure 12: Connection: 1800 exposure time: (a) the overscan is shown on the right and on the bottom with a count intensity of ~ 0. The real image has a an average count intensity in the -10 to 10 range. The histogram of the counts are given in (b).

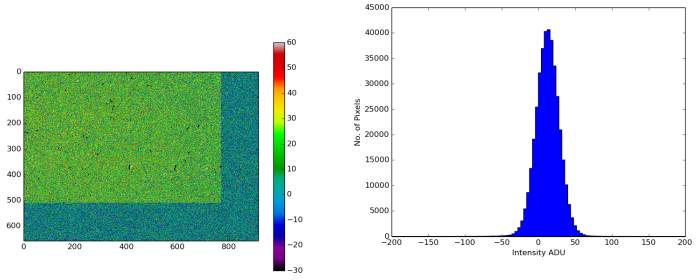

(a) (b)

Figure 13: Groove: 1800 seconds exposure time : (a) the overscan is shown on the right and on the bottom with a count intensity of ~ 0. The real image has an average count intensity in the -10 to 40 range. The histogram of the counts are given in (b).

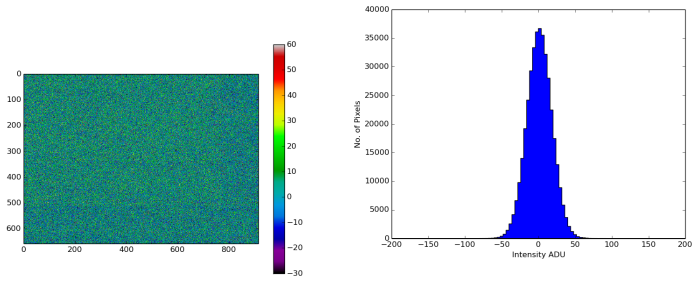

(a) (b)

Figure 14: Groove: 180 seconds exposure time:a) the overscan is shown on the right and on the bottom with a count intensity of ~ 0. The real image has an average count intensity in the -10 to 20 range. The histogram of the counts are given in (b).

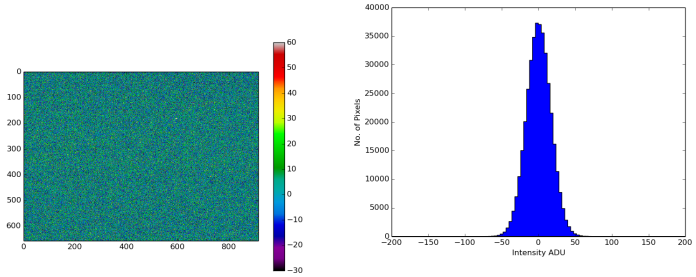

(a) (b)

Figure 15: Connection: 18 seconds exposure time: a) the overscan is shown on the right and on the bottom with a count intensity of ~ 0. The real image has an average count intensity ~ 0. The histogram of the counts are given in (b).

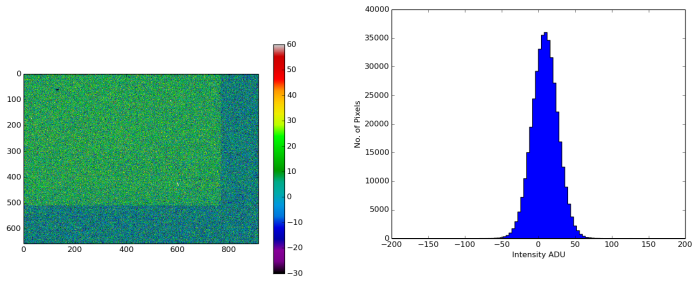

(a) (b)

Figure 16: Shutter: 300 seconds exposure time: a) the overscan is shown on the right and on the bottom with a count intensity in the range of -10 and 40. The real image has an average count intensity in the -10 to 40 range. The histogram of the counts are given in (b).

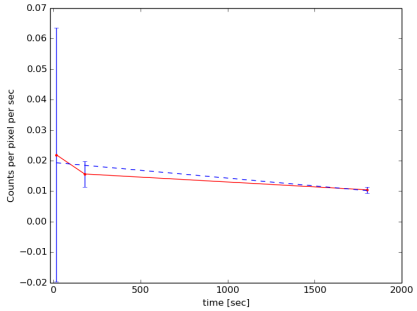

(a) photons/pixel/second plotted as a function of time

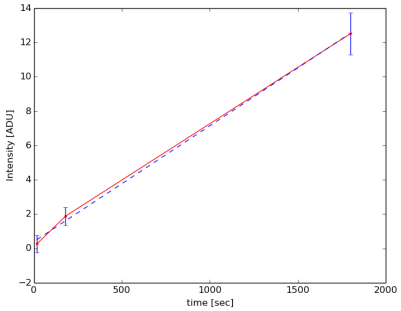

(b) counts [ADU] plotted as a function of time

Figure 17

As shown in figure 17a the calculated photons per pixel per second is constant taking

error into account. The graph has a slope of -5.1×10^{-6} photon per pixel.

As shown in figure 17b the average count mean increase with time. This is as expected as time was increase more photons could can enter causing more counts. The slope of the graph was 0.00675 counts per second.

7 Vacuum pump

To avoid a scattering or absorption of the laser beams inside the cavity a vacuum is needed. For ALPS-II two different types of getter pumps will be used to achieve a vacuum in the two cavity. An ion getter pump will be used on the production cavity. An ion getter pump emits photons (see reference [11]) while a Non-Evaporable getter (NEG) pump does not. For this reason a NEG pump will be used on the regeneration side.

7.1 Types of Vacuum pump

Ion getter pumps ionizes gas molecule cause them to be attached to the cathode electrode and thus removed. A electric potential is applied between an anode and a cathode. When an electron collide with a gas molecule it knocks out another electron from the molecule. The positive ions are attached to the titanium cathode and collide with the surface. If the velocity and energy is adequate sputtering occurs i.e. a titanium atom is ejected from the surface of the cathode. These ejected atoms leave a thin layer of titanium on various surfaces in the pump.

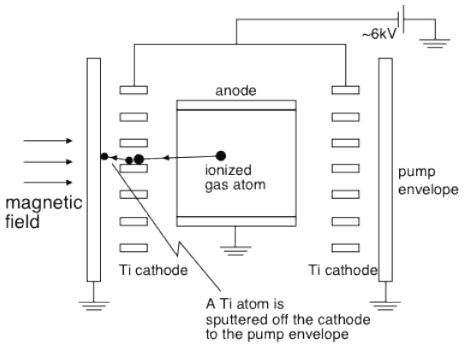

Figure 18: Schematic of an Ion getter pump [8]

A NEG pump contains NEG strips of metal alloys (SAES st707, a reactive zirconium-vanadium-iron powder mixture). This strips are folded to from a more compact pump with a large surface area. The folded strips are known as a wafer module. The st707 reduce the pressure in the chamber by getting or chemically combining atoms to the surface of the getter base material. H_2 diffuses into the getter material and forms a solid

solution which is released when it is heated.

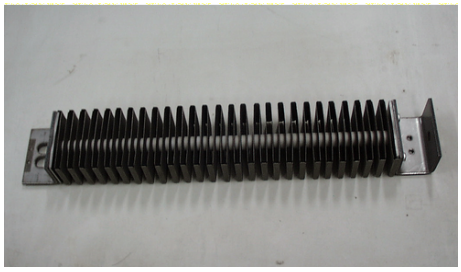

Figure 19: Module of a NEG pump [9]

Sievert's Law describes the relationship between H_2 solid within its NEG and its equilibrium pressure as:

$$\log P = A + 2\log q - \frac{B}{T} \tag{9}$$

where q is the H_2 concentration, P is the equilibrium pressure, T is the getter temperature and A and B are constants for different NEG alloys.

The NEG pump only remove active gases such as CO_2, CO, N_2. The chemical bonds of the gas molecules are bonded on the surface of the NEG and the atoms are chemisorbed forming oxides, nitrides and carbides. Heating the chamber to high temperatures causes the diffusion of atoms into the bulk of the NEG. On the surface of the NEG water vapour and hydrocarbons are split into smaller molecules.

NEG pumps can not absorb and thus do not remove noble gases molecules and therefore if this gases need to be remove the NEG pump needs to be combined with a turbo molecular pump.

The custom built NEG/Ion getter pump would be an ideal vacuum pump for the ALPS experiment. The turbo molecular pump would be turned on first, removing any gases and would reduce the pressure to $\sim 10^{-6}$mbar. It is only when this pressure is reached that the NEG pump could be turn on and thea turbo molecular pump would turned off. The NEG pump would further reduce ther pressure to $\sim 10^{-9}$mbar. As the NEG pump does not produce light this pump could be used during readings and not effect the results.

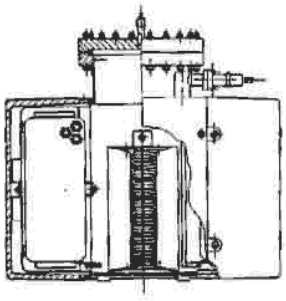

(a) schematic view inside the NEG pump with ion-getter pump cells on left. [10]

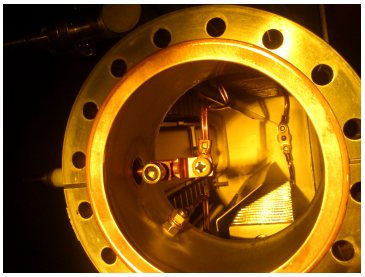

(b) Inside the NEG \ion-getter pump pump

7.2 Testing the NEG pump

To test if the NEG pump would be suitable to use to for the experiment. The pump was first set up out side the lab as shown in figure 21 and a Turbo-molecular pump station was connected.

The Turbo-molecular pump was first activated, reducing the pressure to $\sim 10^{-7}$mbar by removing gas molecules. Once this pressure was achieved the pump was heated in order to heat the reactive zirconium-vanadium-iron powder mixture of the NEG pump. To achieve this an 35A current was applied to the pump. Once the pump was at about 400C the pump was switched on and left to run.

The pump achieved about 10^{-10}mbar which the highest possible pressure. By achieving this pressure the NEG pump is suitable for the regeneration cavity.

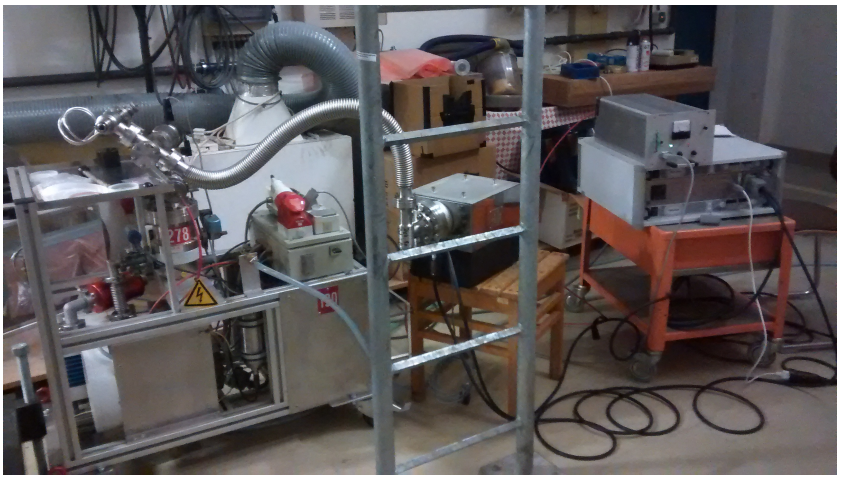

Figure 21: The set up of the NEG/Ion pump and turbo-molecular pump station(from left to right).

8 Conclusion

It was shown that the groove is not light tight. However this result might be by the result of the breadboard is not perfectly parallel to the box.

The shutter was not light-tightness as the light leaked in an order of magnitude more than that of the groove light-tightness test and three orders more that the connection on its own.

The light source constancy test showed that the bulbs intensity did not fluctuate over time and that light-leakage was linearly proportional to the exposure time. The time dependency test show that the number photons entering the shutter box increased at a rate of 0.00675 counts/second.

As the NEG pump reached the maximum pressure the next step is to attached the pump to the pumping port of the regeneration cavity.

9 Acknowledgements

I want to thank my supervisor Babette Döbrich and Dieter Trines for showing me how to set up the NEG pump. I also want to thank Noemie Bastidon, Jan Dreyling-Eschweiler, Jan Hendirk Pold, Reza Hodajerdi,Dieter Horns, Friederike Januschek, Axel Lindner, Andreas Ringwald, Jan Eike von Seggern, Richard Stromhagen and Severin Wipf.

References

[1] P.Sikivie, Experimental Test of the "Invisivle" Axion , Phys. Rev.Lett 51, 1415 (1983)

[2] W. Wuensch et al., Results of a laboratory search for cosmic axions and other weakly coupled light particles,Phys. Rev.D 40 3153 (1989)

[3] M. Ahlers, H. Gies, J. Jaeckel, J. Redondo, A. Ringwald, Light form the Hidden Sector Phys. Rev. D, 76 (2007)

[4] A.Mirizzi, G.G.Raffelt,P.D.Serpico Photon-Axion Conversion in Intergalactic Magnetic Fields and Cosmological Consequences

[5] Carosi, van Bibber, Pivovaroff, Contemp ,The Search for Axions, Phys. 49, No. 4, (2008)

[6] http://alps.desy.de/e141063 reviewed 9/9/2014

[7] Any Light Partial Search II Technical Report

[8] http://philiphofmann.net/ultrahighvacuum/ind_ionpump.html reviewed 9/9/2014

[9] http://www-acc.kek.jp/WWW-ACC-exp/KEKB/VA/pump_files/moduleNEG.gif reviewed 9/9/2014

[10] http://www.aiv.it/portfolio-items/gettering-and-ion-pumping-2/ reviewed 9/9/2014

[11] S. Wipf Bachelor Thesis Light Emission of an Ion Getter Pump in Connection with the ALPS-IIEXPERIMENT 2013

Appendix

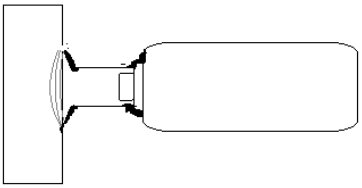

Figure 22: Schematic diagram of the connection with semi-circle lines show the thread attaching the connection to the camera and thicker lines showing were black tape was placed

CCD	
CCD	Kodak KAF-0402ME
Pixel Array	765 x 510 pixels
CCD Size	6.9 x 4.3 mm
Total Pixels	390,000
Pixel Size	9 x 9 microns
Full Well Capacity	~100,000e-
Dark Current	1e- / pixel / sec at 0°C
Antiblooming	Optional

Readout Specifications	
Shutter	Electromechanical
Exposure	0.09 to 3600 seconds, 10ms resolution
Correlated Double Sampling	Yes
A/D Converter	16 bits
A/D Gain	1.5e- unbinned, 2.0e- binned 2x2, 3x3 (1.0e- and 1.4e- for ABG CCD)
Read Noise	13.8e- RMS Typical
Binning Modes	1 x 1, 2 x 2, 3 x 3
Pixel Digitization Rates	Up to 800,000 pixels per second with USB 2.0
Full Frame Download	<1 second

System Specifications	
Cooling – enhanced	Single Stage Thermoelectric, Active Fan, -30°C from Ambient Typical
Cooling – standard	Single Stage Thermoelectric, Active Fan, -20°C from Ambient Typical
Temperature Regulation	±0.1°C
Power	12VDC, power supply included
Computer Interface	USB 2.0 (USB 1.1 compatible)
Computer Compatibility	• Windows 98 / 2000 / Me / XP • Mac OSX

Physical Dimensions	
Optical Head	5 x 4 x 2.5 inches (including fan)
CPU	All electronics integrated into Optical Head, No CPU
Mounting	T-Thread, 1.25" nosepieces included
Weight	Approx. 20 oz. (0.6kg)
Backfocus *(C-mount compatible)*	0.69 inches

Figure 23: Spec sheet for the SBIG ST-402ME

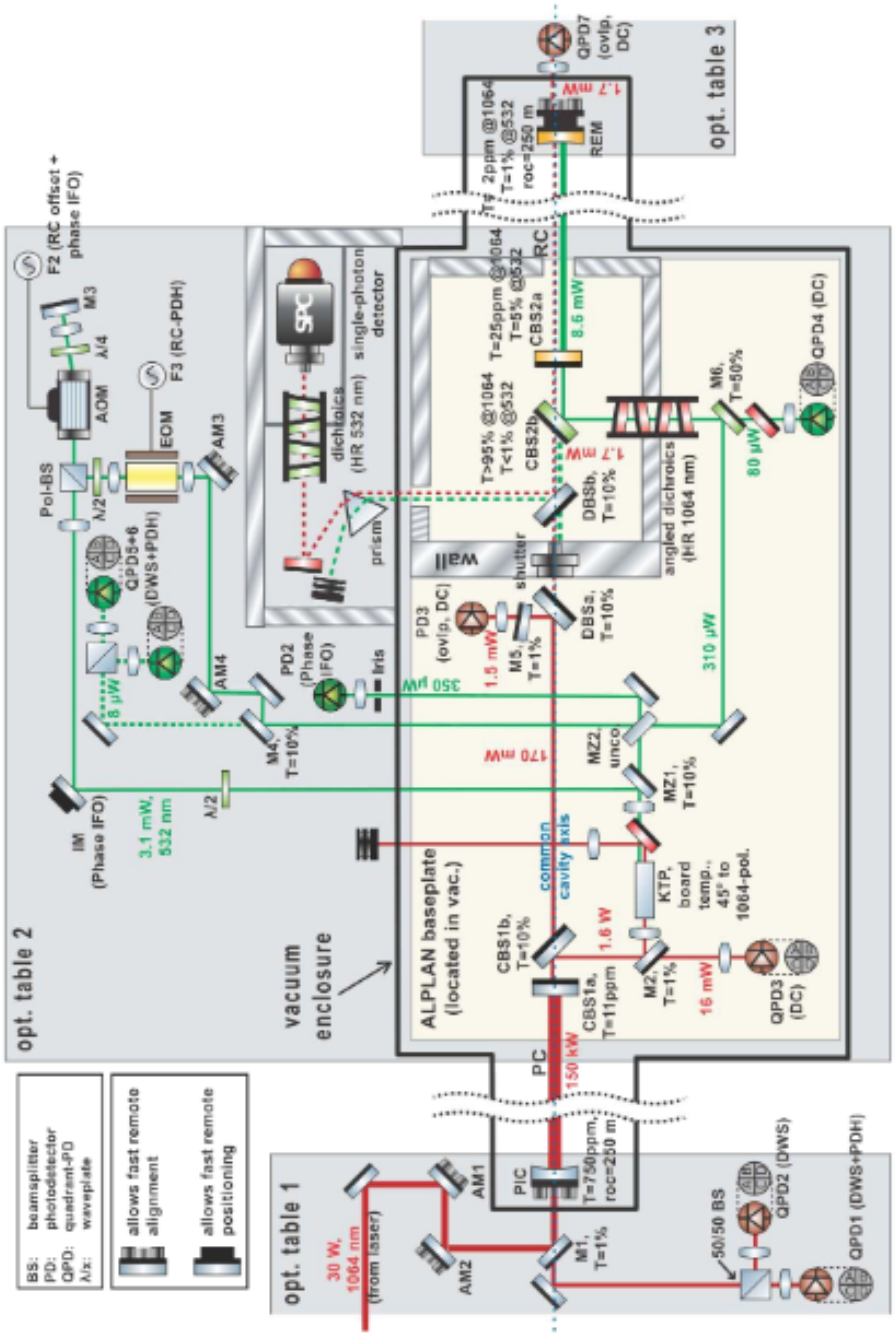

Figure 24: Layout of ALPS-IIc optical tables [7]

Python code to analyse the FIT file taken using CDDOP software

Listing 1: Python code

```
# Python program to load a FITS image and display it

# import needed extensions
from numpy import *
import numpy as np
import matplotlib.pyplot as plt # plotting package
import matplotlib.cm as cm # colormaps
import pyfits
import math


darks = array([pyfits.getdata("1800darkshutter00%d.FIT" % n)
                for n in range(1,10)])

# read in the files
# change the file names as appropriate
h2 = pyfits.open('1800lightconnection001.FIT')
time=1800

n_overscan = 150 # number of overscan columns/lines
safety_margin = 8 # avoid contamination from oscillations at
                  #transition region

def pedestal_correction(image):
    pedestal = image[:,-n_overscan:].mean()
    corr = image - pedestal
    return corr

ch1 = pedestal_correction(darks)
#Master dark frame
MM1 = sum([ch1[0],ch1[1],ch1[2],ch1[3],ch1[4],ch1[5],
                ch1[6],ch1[7],ch1[8]],axis=0)
h1=MM1/9


# copy the image data into a numpy (numerical python) array
h2 = h2[0].data


#nx, ny = h1.shape # find the size of the array
```

```
#print nx , ny

ch1 = pedestal_correction(h1)
ch2 = pedestal_correction(h2)




plt.ion() # do plots in interactive mode
colmap = plt.get_cmap('spectral') # load gray colormap

# plot the first image
plt.figure(1)
plt.imshow(ch1, cmap=colmap) # plot image using gray colorbar
plt.clim(-100,20000)
plt.colorbar()
#plt.show(block=True) # display the image

# plot the second image in another window
plt.figure(2)
plt.imshow(ch2, cmap=colmap) # plot image using gray colorbar
plt.clim(-100,30000)
plt.colorbar()
#plt.show(block=True) # display the image

# find the difference in the images
diff = ch2-ch1

img = diff
img = img[:510,:765]

# plot the difference image
plt.figure(3)
plt.imshow(diff , cmap=colmap) # plot image using gray colorbar
plt.clim(-30,60)
plt.colorbar()
plt.show(block=True) # display the images



# img is a 2-d array, need to change to 1-d to make a histogram
#imgh = 1.0*img # make a copy
nx, ny = img.shape # find the size of the array
imgh = reshape(img, nx*ny) # change the shape to be 1d
```

```
#Getting STD
nx=510
ny=765
FLDmymean2=diff[:nx,:ny]
noPix=nx*ny
FLDmymean1=sum(FLDmymean2)
FLDmymean=FLDmymean1/noPix
FDL1=np.subtract(FLDmymean2,FLDmymean)
FLDstd2=sum(FDL1,axis=0)
FLDstd3=FLDstd2**2
FLDstd4=FLDstd3/noPix
FLDstd=sqrt(FLDstd4)
FLDstdmax=amax(FLDstd)
FLDstdmin=amin(FLDstd)
FLDstdmean=mean(FLDstd)


# print some statistics about the image
print 'Count minimum = ', min(imgh)
print 'Count maximum = ', max(imgh)
print 'Count mean ADU = ', mean(imgh)
print 'Count per pix per sec = ', (mean(imgh)*1.5)/time
print 'Count standard deviation = ', FLDstdmean
print 'Count standard deviation per pix per sec = ',
                                              FLDstdmean*1.5/time


# now plot a histogram of the image values
plt.figure(4)
plt.hist(imgh, bins=100, histtype='stepfilled',range=[-200,200])
plt.xlabel('Intensity ADU')
plt.ylabel('No. of Pixels')
plt.show(block=True) # display the plots
```